AD-A170 978 EFFICIENT ESTIMATION OF PARAMETERS FOR NON-GAUSSIAN AUTOREGRESSIVE PROCESSES(U) RHODE ISLAND UNIV KINGSTON DEPT OF ELECTRICAL ENGINEERING D SENGUPTA ET AL. 1/1

UNCLASSIFIED JUN 86 N00014-84-K-0527 F/G 12/1 NL

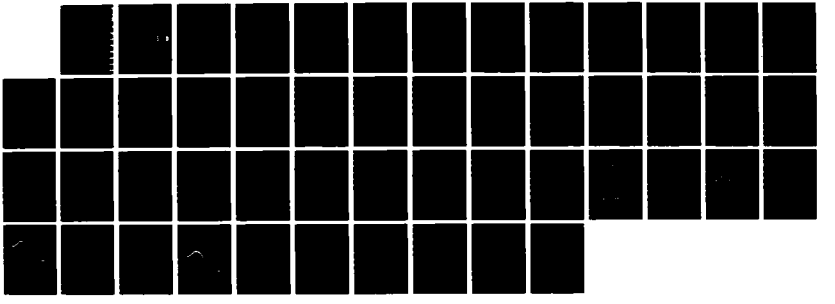

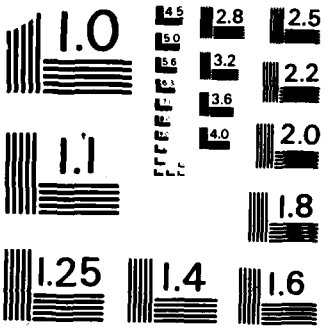

MICROCOPY RESOLUTION TEST CHART
NATIONAL BUREAU OF STANDARDS - 1963 - A

AD-A170 978

Report Number 3

EFFICIENT ESTIMATION OF PARAMETERS FOR NON-GAUSSIAN AUTOREGRESSIVE PROCESSES

DEBASIS SENGUPTA AND STEVEN KAY

Department of Electrical Engineering
University of Rhode Island
Kingston, Rhode Island 02881

DTIC
ELECTE
AUG 1 9 1986
S D
D

June 1986

Prepared for

OFFICE OF NAVAL RESEARCH

Statistic and Probability Branch
Arlington, Virginia 22217
under Contract N00014-84-K-0527
S. M. Kay, Principal Investigator

DTIC FILE COPY

Approved for public release; distribution unlimited

86

SECURITY CLASSIFICATION OF THIS PAGE (When Data Entered)

REPORT DOCUMENTATION PAGE		READ INSTRUCTIONS BEFORE COMPLETING FORM
1. REPORT NUMBER: 3	2. GOVT ACCESSION NO.: AD-A170 978	3. RECIPIENT'S CATALOG NUMBER
4. TITLE (and Subtitle): Efficient Estimation of Parameters for Non-Gaussian Autoregressive Processes		5. TYPE OF REPORT & PERIOD COVERED: August 1984 to July 1986
		6. PERFORMING ORG. REPORT NUMBER
7. AUTHOR(s): Debasis Sengupta and Steven Kay		8. CONTRACT OR GRANT NUMBER(s): N00014-84-K-0527
9. PERFORMING ORGANIZATION NAME AND ADDRESS: Electrical Engineering Department, University of Rhode Island, Kingston, Rhode Island 02881		10. PROGRAM ELEMENT, PROJECT, TASK AREA & WORK UNIT NUMBERS
11. CONTROLLING OFFICE NAME AND ADDRESS: Office of Naval Research, Department of the Navy, Arlington, Virginia 22217		12. REPORT DATE: May 1986
		13. NUMBER OF PAGES: 45
14. MONITORING AGENCY NAME & ADDRESS (if different from Controlling Office)		15. SECURITY CLASS. (of this report): Unclassified
		15a. DECLASSIFICATION DOWNGRADING SCHEDULE

16. DISTRIBUTION STATEMENT (of this Report)

Approved for public release. Distribution unlimited.

17. DISTRIBUTION STATEMENT (of the abstract entered in Block 20, if different from Report)

18. SUPPLEMENTARY NOTES

19. KEY WORDS (Continue on reverse side if necessary and identify by block number)

Parameter Estimation
Non-Gaussian Processes
Cramer-Rao Bounds
Maximum Likelihood Estimator
Autoregressive Processes

20. ABSTRACT (Continue on reverse side if necessary and identify by block number)

The problem of estimating the parameters of a non-Gaussian autoregressive process is addressed. Departure of the driving noise from Gaussianity is shown to have the potential of improving the accuracy of the estimation of the parameters. While the standard linear prediction techniques are computationally efficient, they show a substantial loss of efficiency when applied to non-Gaussian processes. A maximum likelihood estimator is proposed for more precise estimation

DD FORM 1 JAN 73 1473 EDITION OF 1 NOV 65 IS OBSOLETE

SECURITY CLASSIFICATION OF THIS PAGE (When Data Entered)

Abstract

The problem of estimating the parameters of a non-Gaussian autoregressive process is addressed. Departure of the driving noise from Gaussianity is shown to have the potential of improving the accuracy of the estimation of the parameters. While the standard linear prediction techniques are computationally efficient, they show a substantial loss of efficiency when applied to non-Gaussian processes. A maximum likelihood estimator is proposed for more precise estimation of the parameters of these processes coupled with a realistic non-Gaussian model for the driving noise. The performance is compared to that of the linear prediction estimator and as expected the maximum likelihood estimator displays a marked improvement.

COPY INSPECTED

Accesion For
NTIS CRA&I
DTIC TAB
Unannounced
Justification
By
Distribution /
Availability Codes
Dist | Avail and/or Special
A-1

I. Introduction

Estimation of the parameters of a time series model has been a widely addressed problem. Rational transfer function or time series models are the most popular of these.[1] Autoregressive (AR) models are used more often than the moving average and autoregressive moving average models because of the inherent mathematical simplicity.[2] When the driving noise is Gaussian, the maximum likelihood estimator (MLE) is easily found for the AR model under reasonable assumptions.[3]

Although the Gaussian model for the driving noise is appropriate for a wide variety of problems, in some applications it is not. The noise encountered in underwater detection problems is often characterized by the presence of sharp spikes due to ice break-up and offshore drilling.[4],[5] Spikes are also common in the atmospheric noise encountered in low frequency communication systems.[6] The Gaussian model is not flexible enough to incorporate these high-amplitude events mainly because of the sharp roll-off of the probability density function (PDF).

A variety of alternative models have been proposed. A PDF that is appropriate for a non-Gaussian process with "heavy tails" is the Gaussian mixture model

$$f(u) = (1-\varepsilon)E_{B(u)} + \varepsilon E_I(u) , \qquad 0 < \varepsilon < 1 \tag{1}$$

where $E_B(u)$ and $E_I(u)$ are Gaussian PDF's with parameters $[\mu_B, \sigma_B^2]$ and $[\mu_I, \sigma_I^2]$ respectively.[7] Subscripts B and I are used to denote background and interference, respectively. Assuming $\sigma_I^2 \gg \sigma_B^2$, one can allow for a wide range of amplitudes and frequencies of occurence of spikes by appropriately choosing σ_I^2 and ε, the mixture parameter.

Once the driving process is characterized, the AR model can describe a large set of correlation patterns with only a few number of parameters. Most of the natural noise-channels, such as the soil and the sea-water, are low-pass in nature and the processes at their output tend to be well-suited for an AR model.[8],[9]

Physically motivated as the Gaussian mixture model is, it does not enjoy the mathematical simplicity associated with a Gaussian model.[10] For example, the least squares estimator of the AR parameters is no longer a close approximation to the MLE for reasonably large data records. This leads to the problem of finding a good method to estimate the parameters that characterize a mixed-Gaussian AR process. Maximum likelihood estimation is the most widely considered approach for all mixture-density estimation problems.[7]

This paper addresses the problem of maximum likelihood estimation of the parameters of an AR process driven by white noise with a mixed-Gaussian PDF given by (1). As a preliminary step, we

assume μ_B and μ_I to be zero and σ_B^2 and σ_I^2 to be known but ε unknown.

The paper is organized as follows. Section II describes the Cramer-Rao bounds for the parameters of a mixed-Gaussian AR process and attempts to interpret them. Section III points out the inefficiency of least squares estimation by relying on theoretical and experimental results . Section IV formulates the MLE for this problem while section V discusses its performance. Section VI summarizes the results and discusses possible applications of the MLE approach.

II. Cramer-Rao Bounds

The approximate Cramer-Rao bound for the unbiased estimator of the location parameter or mean μ, driving noise variance and autoregressive filter parameters is known for a finite variance p-th order AR process

$$x_n = \mu - \sum_{j=1}^{p} a_j \, (x_{n-j} - \mu) + u_n \qquad (2)$$

if u_n has a symmetric PDF f with variance σ^2 and a_k are the autoregressive filter parameters. The Fisher information matrix for the parameter vector $\underline{\theta} = [\, \mu \; \underline{a}^T \; \sigma^2 \,]^T$, assuming that $\{ x_1, x_2, \ldots x_N \}$ are observed, is given by

$$\underline{I}_\theta = -E \begin{bmatrix} \frac{\partial^2 \ln f}{\partial \mu^2} & \frac{\partial^2 \ln f}{\partial \mu \partial \underline{a}^T} & \frac{\partial^2 \ln f}{\partial \mu \partial \sigma^2} \\ \frac{\partial^2 \ln f}{\partial \underline{a} \partial \mu} & \frac{\partial^2 \ln f}{\partial \underline{a} \partial \underline{a}^T} & \frac{\partial^2 \ln f}{\partial \underline{a} \partial \sigma^2} \\ \frac{\partial^2 \ln f}{\partial \sigma^2 \partial \mu} & \frac{\partial^2 \ln f}{\partial \sigma^2 \partial \underline{a}^T} & \frac{\partial^2 \ln f}{\partial \sigma^{2\,2}} \end{bmatrix}$$

which may be shown to be approximately[11],[12]

$$\underline{I}_\theta = (N - p) \begin{bmatrix} (1 + \sum_{j=1}^{p} a_j)^2 I_f & \underline{0}_p^T & 0 \\ \underline{0}_p & I_f \underline{C} & \underline{0}_p \\ 0 & \underline{0}_p^T & I_{\sigma^2} \end{bmatrix} \tag{3}$$

where $\underline{a} = [a_1 \; a_2 \; \ldots \; a_p]^T$

$$I_f = E\left\{ \left[\frac{\partial}{\partial u} \ln f(u) \right]^2 \right\}$$

$$I_{\sigma^2} = \frac{1}{4\sigma^4} \left[E\left\{ \left[u \frac{\partial}{\partial u} \ln f(u) \right]^2 \right\} - 1 \right]$$

$\underline{0}_p$ is a pxl vector of zeroes and $\underline{C}$ is the pxp covariance matrix of the time series. This result is asymptotic (true for large data records) because the contribution of the first p samples has been ignored.[12] No results are available for finite data records.

It is of interest to explicitly determine I_f and I_{σ^2} for a Gaussian distribution. In this case

$$\ln f(u) = -\frac{1}{2} \ln(2\pi) - \ln\sigma - \frac{1}{2\sigma^2} u^2$$

$$\frac{\partial}{\partial u} \ln f(u) = -\frac{u}{\sigma^2}$$

$$I_f = E\left\{ \left[\frac{\partial}{\partial u} \ln f(u) \right]^2 \right\} = \frac{1}{\sigma^4} E[u^2] = \frac{1}{\sigma^2} \tag{4}$$

$$I_{\sigma^2} = \frac{1}{4\sigma^4}\left[E\left\{ \left[-\frac{u^2}{\sigma^2} \right]^2 \right\} - 1 \right] = \frac{1}{4\sigma^4}\left[\frac{3\sigma^4}{\sigma^4} - 1 \right] = \frac{1}{2\sigma^4} \tag{5}$$

Substitution of (4) and (5) into (3) produce the well known results for the CR bounds for Gaussian AR processes.[13] These results will be useful later.

Returning to the general non-Gaussian case, we are interested in determining the CR bounds for $\underline{a}$ and σ^2 only. μ is assumed to be known and equal to zero. The block-diagonal nature of I_θ makes it possible to invert it by inverting each block. Therefore, the covariance matrix of an unbiased estimator $\hat{\underline{a}}$ of $\underline{a}$ is bounded by

$$\mathrm{Cov}(\hat{\underline{a}}) \geq \frac{1}{I_f}\left[\frac{\underline{C}^{-1}}{N-p} \right] = \frac{1}{\sigma^2 I_f}\left[\frac{\underline{C}_n^{-1}}{N-p} \right] \tag{6}$$

while the matrix inequality means that the difference of the right and left side matrices is positive semidefinite. $\underline{C}_n$ is the "normalized" covariance matrix obtained by dividing $\underline{C}$ by σ^2 so that $\underline{C}_n$ depends only on the AR filter parameters. It can be noted from (4) that in the Gaussian case $\sigma^2 I_f$ is unity and the CR bound for $\underline{a}$ becomes $\sigma^2 \underline{C}^{-1}(N-p) = \underline{C}_n^{-1}/(N-p)$ in accordance with known results.[3]

For a fixed variance σ^2 the factor I_f is smallest and hence <u>the AR filter parameters are most difficult to estimate in the Gaussian case</u>. This can be shown easily from the Cauchy-Schwartz inequality

$$I_f\sigma^2 = E\left\{\left[\frac{f'(u)}{f(u)}\right]^2\right\} E\left[u^2\right] \geq \left| E\left[\frac{f'(u)}{f(u)}\, u\right]\right|^2$$

$$= \left| \int_{-\infty}^{\infty} \frac{f'(u)}{f(u)}\, u\, f(u)\, du \right|^2$$

$$= \left| \int_{-\infty}^{\infty} f'(u)\, u\, du \right|^2$$

$$= \left| \left[u\, f(u) - \int_{-\infty}^{u} f(t)\, dt\right] \Big|_{-\infty}^{\infty} \right|^2$$

$$= \left| u\, f(u) \Big|_{-\infty}^{\infty} - \int_{-\infty}^{\infty} f(u)\, du \right|^2$$

$$= |\, 0-1\,|^2$$

$$= 1$$

Hence

$$I_f \geq \frac{1}{\sigma^2} \tag{7}$$

Note that equality holds for a Gaussian distribution, as shown in (4). For any other symmetric distribution with variance σ^2, I_f is larger than this minimum value. In fact the Gaussian PDF is the unique PDF satisfying the equality. To show this consider zero mean random variables A and B where $A = f'(u)/f(u)$ and $B = u$. Then if (7) holds with equality

$$E(A^2)E(B^2) = [\, E(AB)\,]^2$$

This implies that

$$\frac{E(A^2)}{E(AB)} = \frac{E(AB)}{E(B^2)} = c$$

where c is some constant.

Therefore $E(A^2) = cE(AB) = c^2E(B^2)$

ie, $E(A^2) + c^2E(B^2) - 2cE(AB) = 0$

ie, $E(A^2 - 2cAB + c^2B^2) = 0$

ie, $E(A - cB)^2 = 0$

ie, $\int_{-\infty}^{\infty} (A - cB)^2 f(u)\, du = 0.$

$f(u)$ and $(A - cB)^2$ are both non-negative over the whole range of integration. Since we are only interested in A and B for those values of u which have non-zero probability, $(A - cB)^2$ has to be identically zero over the whole domain of f.

Therefore $A = cB$

This equality implies

$$\frac{f'(u)}{f(u)} = cu, \qquad -\infty < u < \infty$$

Integrating both sides yields

$$\ln f(u) = cu^2/2 + \ln K \quad \text{(where K is some constant)}$$

ie, $f(u) = K\exp(cu^2/2)$.

This is a normal distribution with mean 0 and variance $-1/c$.

(7) allows us to compare the CR bounds for $\hat{\underline{a}}$, as given by (6), for any symmetric PDF of the driving noise to that for the Gaussian driving noise. An obvious implication of (7) is that it is possible to estimate the AR parameters more precisely in the non-Gaussian case than in the Gaussian case. In summary,

$$\text{Cov}\,(\hat{\underline{a}}) \geq \frac{1}{\sigma^2 I_f} \cdot \frac{1}{N-p}\, \underline{C}_n^{-1} \qquad \text{in the non-Gaussian case}$$

$$\text{and} \quad \text{Cov}\,(\hat{\underline{a}}) \geq \frac{1}{N-p}\, \underline{C}_n^{-1} \qquad \text{in the Gaussian case} \qquad (8)$$

I_f has another interpretation. It is the Fisher information for the estimator of the mean or the location parameter of a univariate PDF. This may be observed by setting $a_j=0$, $j=1,2,\ldots,p$ in the (1,1) element of $\underline{I}_\theta$ as given in (3) and noting that the factor (N-p) is due

to accumulation of information from (N-p) samples, ignoring the contribution of the first p samples. The result also holds for the mean of AR processes except for a multiplying constant. This means that given two AR processes having identical power spectral densities but different PDF's of driving noise with equal variances, it will be easier to estimate the AR filter parameters of that process for which estimation of the mean is easier. For the specific case of a zero mean Gaussian mixture model described in (1)

$$\sigma^2 = (1-\varepsilon)\sigma_B^2 + \varepsilon\sigma_I^2 \tag{9}$$

σ_B^2 and σ_I^2 are assumed to be known. I_f can be computed in this case as follows:

$$\text{Let} \quad F_B(u) = \frac{1-\varepsilon}{\sqrt{2\pi\sigma_B^2}} \exp\left[-u^2/2\sigma_B^2 \right] \tag{10a}$$

$$\text{and} \quad F_I(u) = \frac{\varepsilon}{\sqrt{2\pi\sigma_I^2}} \exp\left[-u^2/2\sigma_I^2 \right] \tag{10b}$$

$$\text{Then} \quad f(u) = F_B(u) + F_I(u)$$

$$f'(u) = -u \left[F_B(u)/\sigma_B^2 + F_I(u)/\sigma_I^2 \right]$$

$$= -u \left[G_B(u) + G_I(u) \right]$$

$$\text{where} \quad G_B(u) = F_B(u)/\sigma_B^2 \quad \text{and} \quad G_I(u) = F_I(u)/\sigma_I^2 \tag{11}$$

$$I_f = \int_{-\infty}^{\infty} \frac{[f'(u)]^2}{f(u)}\, du = \int_{-\infty}^{\infty} \frac{\left[u(G_B(u)+G_I(u))\right]^2}{F_B(u)+F_I(u)}\, du \tag{12}$$

This integral can be evaluated using standard numerical techniques. $\sigma^2 I_f$ can be thought of as an index of non-Gaussianity where positive departures from 1 indicate a higher degree of non-Gaussianity as far as the estimation of the AR filter parameters is concerned. Figure 1 plots $\log(\sigma^2 I_f)$ vs. ε for $\sigma_B^2 = 1$, $\sigma_I^2 = 1000$ and $\sigma_B^2 = 1$, $\sigma_I^2 = 100$. For $\varepsilon = 0$ and $\varepsilon = 1$ the distribution degenerates to a Gaussian one with variance σ_B^2 and σ_I^2, respectively. In both these cases $\log(\sigma^2 I_f) = 0$. The plot shows how much improvement can be expected in the preciseness of the estimation of AR filter parameters for different values of ε. For example, for $\varepsilon = 0.1$, $\sigma_B^2 = 1$ and $\sigma_I^2 = 1000$, the covariance matrix is scaled down from the Gaussian case by a factor of about 100. We will be primarily interested in values of $\varepsilon < 0.2$.

The CR bound on variance can also be computed numerically. From (3) it is evident that

$$\mathrm{Var}(\hat{\sigma^2}) \geq \frac{1}{(N-p) I_{\sigma^2}}$$

$$\text{where} \quad I_{\sigma^2} = \frac{1}{4\sigma^4} \left[\int_{-\infty}^{\infty} \frac{u^2 [f'(u)]^2}{f(u)} \, du \quad - \quad 1 \right]$$

For the Gaussian mixture model this becomes

$$I_{\sigma^2} = \frac{1}{4\sigma^4} \left[\int_{-\infty}^{\infty} \frac{u^4 \left[G_B(u) + G_I(u) \right]^2}{F_B(u) + F_I(u)} \, du \quad - 1 \right] \tag{13}$$

using notations of (10) and (11). The integral can be evaluated numerically.

Figures 2 and 3 show two typical non-Gaussian autoregressive time series along with the driving noise time series. They provide some insight as to why it should be possible to estimate the AR parameters more precisely in the non-Gaussian case. The Gaussian mixture model is characterized by the presence of large spikes in the driving noise time series (Figures 2a, 3a), due to the high variance Gaussian component. The spikes act as impulses to the input of the AR filter and result in "ringing" at the output (Figures 2b, 3b). This ringing is actually the impulse response of the filter which temporarily dominates the low variance component at the output. It is probably these impulse responses that carry additional information about the filter parameters.

III. Least Squares Techniques

The usual AR parameter estimation techniques (eg, Autocorrelation, Covariance, Forward-backward etc.)[2] do not enjoy the property of asymptotic efficiency in the non-Gaussian case. Although they are still computationally efficient, they perform much poorer than the MLE.

Two typical AR(4) processes[2] have been chosen for computer simulations. The parameters are given in Table I. σ^2 is assumed to be unity for both processes. Process I is broadband while process II is

narrowband. 50 Forward-backward spectral estimates have been plotted for these two processes in Figure 4. The sample means and sample variances of $\hat{\underline{a}}$ and $\hat{\sigma}^2$ have been listed and compared against the CR bounds in Table II.(The performance of the MLE will be described in section IV.) The results are based on 500 experiments with 1000 data samples in each. σ_B^2 and σ_I^2 are equal to 1 and 100 respectively. Also the mixture parameter is $\varepsilon = 0.1$. The AR process was generated by passing a white mixed-Gaussian process through a filter, allowing sufficient time for the transients to decay. The white process was generated by randomly selecting from two mutually independent white Gaussian processes with PDF's $E_B(u)$ and $E_I(u)$ (having variances σ_B^2 and σ_I^2 respectively) on the basis of a series of Bernoulli trials with probability of success ε. Thus a random variable can be expected to come from population I for $(1-\varepsilon)$ fraction of times and from population II for ε fraction of times so that the overall distribution is as given in (1).

The CR bounds for the Gaussian case (see (8)) have also been listed in table II. As expected, the bound for the AR parameters in the Gaussian case is much higher than those in the non-Gaussian case. It is interesting to note that the performance of the Forward-backward estimator approaches the Gaussian CR bound. This confirms the well known result that the least squares estimates are asymptotically Gaussian with mean equal to the true parameters and covariance matrix equal to the Gaussian CR bound.[13] However, as will be shown in in

section V, the MLE attains the true CR bound, better by a factor of 10 in accordance with Figure 1b.

Clearly, the Forward-backward estimator, which is typical of all least squares methods, can not take advantage of the presence of the "contaminating" process. The performance of the covariance method was found to be about the same. (The exact results for the covariance method has not been reported here.) This confirmation of the expected inefficiency of the least squares techniques[12],[14] calls for the use of a more efficient method which will be able to exploit the reduction in the CR bounds. One such method is the MLE which is discussed in the next section.

IV. Maximum Likelihood Estimation

In this section a Newton-Raphson search algorithm is proposed for the (p+1)-dimensional maximization of the conditional likelihood function. The likelihood function is given by the joint PDF of the observed AR process which can be obtained from the joint PDF of the driving noise as follows. An AR(p) time series is linearly related to the driving noise time series

$$u_n = \sum_{j=0}^{p} a_j x_{n-j} \tag{14}$$

where the identification $a_0 = 1$ has been made. This is just another way

of writing (2), which makes it possible to determine the conditional likelihood function of $[\, x_1\ x_2\ \ldots\ x_N \,]^T$ in terms of the joint distribution f of $\underline{u} = [\, u_{p+1}\ u_{p+2}\ \ldots\ u_N \,]^T$. The transformation is

$$\begin{bmatrix} u_{p+1} \\ u_{p+2} \\ \vdots \\ u_N \end{bmatrix} = \underbrace{\begin{bmatrix} 1 & & & & & \\ a_1 & 1 & & & & \\ \vdots & \ddots & \ddots & & & \\ a_p & \cdots & a_1 & 1 & & \\ 0 & & \ddots & \ddots & \ddots & \\ \vdots & & & & & \\ 0 & \cdots & 0 & a_p & \cdots & 1 \end{bmatrix}}_{\underline{A}} \begin{bmatrix} x_{p+1} \\ x_{p+2} \\ \vdots \\ x_N \end{bmatrix} + \begin{bmatrix} \sum_{j=1}^{p} x_j a_{p+1-j} \\ \sum_{j=2}^{p} x_j a_{p+2-j} \\ \vdots \\ x_p a_p \\ 0 \\ \vdots \\ 0 \end{bmatrix}$$

The Jacobian of the transformation from $[\, x_{p+1}\ x_{p+2}\ \ldots\ x_N \,]$ to $\underline{u}$ is just $\underline{A}$. The determinant of the Jacobian is unity so that the joint PDF f of $[\, x_{p+1}\ x_{p+2}\ \ldots\ x_N \,]$ given $x_1, x_2, \ldots x_p$ is

$$f(x_{p+1}, x_{p+2}, \ldots x_N \mid x_p, x_{p-1}, \ldots x_1) = f(\, \underline{u}(\underline{x}) \,) = \prod_{n=p+1}^{N} f(u_n(\underline{x}))$$

$$f(\underline{u}) = \prod_{n=p+1}^{N} f(u_n) = \prod_{n=p+1}^{N} \left[\frac{(1-\varepsilon)}{\sqrt{2\pi\sigma_B^2}} \exp\left[-\frac{u_n^2}{2\sigma_B^2} \right] + \frac{\varepsilon}{\sqrt{2\pi\sigma_I^2}} \exp\left[-\frac{u_n^2}{2\sigma_I^2} \right] \right]$$

Then $f(x_{p+1}, x_{p+2}, \ldots x_N \mid x_p, x_{p-1}, \ldots x_1)$

$$= \prod_{n=p+1}^{N} \left[\frac{(1-\varepsilon)}{\sqrt{2\pi\sigma_B^2}} \exp\left[-\frac{1}{2\sigma_B^2} \left(\sum_{j=0}^{p} a_j x_{n-j} \right)^2 \right] + \frac{\varepsilon}{\sqrt{2\pi\sigma_I^2}} \exp\left[-\frac{1}{2\sigma_I^2} \left(\sum_{j=0}^{p} a_j x_{n-j} \right)^2 \right] \right]$$

A Newton-Raphson iteration step for $\underline{\theta} = [\, \underline{a}^T\ \sigma^2 \,]^T$ is

$$\underline{\theta}_{i+1} = \underline{\theta}_i - \underline{H}^{-1}\underline{G} \tag{15}$$

where $$\underline{G} = \left[\frac{\partial \ln f}{\partial a_1} \quad \frac{\partial \ln f}{\partial a_2} \quad \cdots \quad \frac{\partial \ln f}{\partial a_p} \quad \frac{\partial \ln f}{\partial \sigma^2} \right]^T \tag{16}$$

and $$\underline{H} = \begin{bmatrix} \frac{\partial^2 \ln f}{\partial a_1^2} & \cdots & \frac{\partial^2 \ln f}{\partial a_1 \partial a_p} & \frac{\partial^2 \ln f}{\partial a_1 \partial \sigma^2} \\ \vdots & & \vdots & \vdots \\ \frac{\partial^2 \ln f}{\partial a_p \partial a_1} & \cdots & \frac{\partial^2 \ln f}{\partial a_p^2} & \frac{\partial^2 \ln f}{\partial a_p \partial \sigma^2} \\ \frac{\partial^2 \ln f}{\partial \sigma^2 \partial a_1} & \cdots & \frac{\partial^2 \ln f}{\partial \sigma^2 \partial a_p} & \frac{\partial^2 \ln f}{\partial \sigma^{2\,2}} \end{bmatrix} \tag{17}$$

Appendix A gives a detailed derivation of the entries of $\underline{G}$ and $\underline{H}$. Although the expansions are complicated, they exhibit some structure. This would allow partly concurrent computation of the gradient and hessian entries in each step of Newton-Raphson iterations. The estimates from the Forward-backward method can serve as initial estimates.

For large data records the Hessian, evaluated at the true values of the parameters, approaches the negative of the Fisher information matrix by the law of large numbers.[16] The Fisher information matrix is known to be positive definite. Therefore the negative of the Hessian will be positive definite when the parameter vector is close to its true value. Since the MLE is consistent, the maximum of the likelihood function is expected to occur close to the true value of the parameter vector. Hence the Hessian will be negative definite in the neighborhood

of the maximum of the likelihood function, implying that the function is convex in that region. This property of the Hessian can be utilized to avoid the matrix inversion required by (15) in the following way. Rewriting (15) as

$$(-\underline{H})\underline{\theta}_{i+1} = (-\underline{H})\underline{\theta}_i + \underline{G} \tag{18}$$

it is possible to compute the right hand side from $\underline{\theta}_i$. Thus (18) is a set of linear equations which can be solved by a Cholesky decomposition.

The first and second order derivatives should be scaled by 1/N in order to avoid the possibility of the terms growing unmanageably large. The motivation for scaling down the terms is best understood by considering the case of optimization over a single parameter assuming the other parameters to be known. The Fisher information, which is a diagonal element of $\underline{I}_{\theta}$ as given by (3), increases as N increases. $\underline{H}$ (a scalar in this case) also increases accordingly, being of the order of the Fisher information in magnitude, and has to be scaled down. Multidimensional optimization would be even more difficult without scaling.

A difficulty in obtaining convergence of the Newton-Raphson iteration is the apparent weak dependence of the likelihood function upon σ^2 (or equivalently, ε). A transformation has been successfully

used to circumvent this difficulty. Appendix B addresses this problem in detail.

While the theoretical proof of convexity of the likelihood function for finite data records is not available, the simulations seem to support this. The results of the simulations are discussed in the following section.

V. Computer Simulations of the Performance of the MLE

The least squares estimates obtained by the Forward-backward method were chosen as initial iterates for the Newton-Raphson iteration required to find the MLE. An error criterion was defined and the iteration was considered to have converged if the criterion was satisfied. A maximum of 100 iterations was allowed. The error criterion was

$$\sum_{j=1}^{p+1} \left| \frac{\theta_j^i - \theta_j^{i-1}}{\theta_j^i} \right| < R$$

where θ_j^i is the ith iterate for the jth element of $\underline{\theta}$. R can be chosen on the basis of on-line experience about the percentage of realizations that converge for a given value of R. $R=10^{-3}$ seemed to work well in the cases reported here. A transformation on ε (described in Appendix B)

was used to enhance convergence, as was mentioned in section IV. Typically the iterations converged in 4-6 steps and less than 1% of them failed to converge. The results to be described do not reflect the experiments resulting in failure to convergence.

50 realizations of the MLE spectral estimator for the two typical AR(4) processes described in section III have been plotted in Figure 5. While it shows only moderate improvement upon the Forward-backward estimates plotted in Figure 4, it should be noted that Figure 5a has less crossovers than Figure 4a. This suggests that the variability of σ^2 might be the major factor behind scattering the plots apart, an explanation confirmed by Figures 6 and 7 which compare the two methods with the estimate of the variance replaced by the true variance. They indicate a considerable improvement for the MLE while the Forward-backward estimates improve only slightly.

Table III compares the sample mean and sample variance of the MLE estimators based on 500 experiments to the CR bound. The number of data points in each experiment is 1000. The maximum likelihood estimators indeed appear to be efficient except for the estimator of variance which displays a much higher variability than the CR bound.

Estimating σ^2 in this case is equivalent to estimating ε, which represents the fraction of times the high variance Gaussian component appears in the observed data. It is comprehensible that for small ε

this estimation will suffer from the difficulties associated with determining the probabilities of rare events. Very large data records will be necessary to have a reasonably good estimate. Apparently, N=1000 was not large enough in this case. However it should be mentioned that the difficulty in estimating the driving noise power may not be important in some applications. For example, in some detection problems it is possible to make hypothesis tests invariant to σ^2. [15]

Although convergence was not a major problem for N=1000, shorter data records did exhibit more sensitivity to initial conditions. The reason is attributed to the possible non-quadratic nature of the log likelihood function which makes convergence of the Newton-Raphson iteration more difficult.

VI. Summary

The Cramer-Rao bound for the estimators of the parameters of non-Gaussian AR processes was observed to be less than that for Gaussian AR processes. The performance of the popular least squares or linear prediction techniques however only achieve the Gaussian CR bound. The MLE technique, although computationally intensive compared to standard linear prediction approaches, yields more accurate estimates for non-Gaussian AR processes. Simulation results indicate that the MLE is asymptotically efficient. It appears to be a viable approach for parameter and spectral estimation of non-Gaussian AR processes and may also be applicable to linear prediction of time

series and detection of signals in noise. Future work will address means to reduce the computational burden of the MLE. Also, the extension of this work to the case of unknown ratio of background and interfering noise powers will be studied.

References:

1) S.M. Kay and S.L. Marple,Jr., "Spectrum Analysis - A Modern Perspective", Proc. IEEE, pp. 1380-1419, Nov.1981.

2) S.M. Kay, Modern Spectral Estimation: Theory and Application, Chapters 5-7, Prentice-Hall, to be published.

3) G.E.P. Box and G.J. Jenkins, Time Series Analysis: Forecasting and Control, Chapter 7, San Francisco: Holden-Day, 1970.

4) J.S. Wit, "Advances in Antisubmarine Warfare", Scientific American, pp. 31-41, Vol.244, No.2, Feb.1981.

5) R.F. Dwyer, "Fram II Single Channel Ambient Noise Statistics", NUSC TR 6583, New London, Conn., Nov.1981.

6) S.L. Bernstein et al., "Long-range Communication at Extremely Low Frequency", Proc. IEEE, pp. 292-312, Vol. 62, Mar.1974.

7) R.A. Render and H.F. Walker, "Mixture Densities, Maximum Likelihood and the EM Algorithm", SIAM Review, pp. 195-239, Vol.26, No.2, April 1984.

8) R. Urick, Principles of Underwater Sound for Engineers, Chapter 7, New York: McGraw Hill, 1967.

9) W.C. Knight, R.G. Pridham and S.M. Kay, "Digital Signal Processing for Sonar", Proc. IEEE, pp. 1451-1506, Nov.1981.

10) Sir M. Kendall and A. Stuart, The Advanced Theory of Statistics Vol. II, Chapters 18-19, New York: Macmillan Publishing, 1979.

11) D.R. Cox and D.V. Hinkley, Theoretical Statistics, Chapter 4, London: Chapman and Hall, 1974.

12) R.D. Martin, "The Cramer-Rao Bound and Robust M-estimates for

Autoregressions", Biometrika, pp. 437-442, Vol. 69, No. 2, 1982.

13) T.W. Anderson, The Statistical Analysis of Time Series, Chapter 5, New York: John Wiley, 1971.

14) D.R. Cox and D.V. Hinkley, "A Note on the Efficiency of the Least Squares", J.R. Statist. Soc., B 30, 284-289, 1968.

15) E.L. Lehmann, Testing Statistical Hypotheses, New York: John Wiley, 1959.

APPENDIX A

Computation of Gradient and Hessian in Newton-Raphson iterations

From section IV, the approximate (conditional) log likelihood function can be written as

$$\ln f = \sum_{n=p+1}^{N} \ln \left[\frac{(1-\varepsilon)}{\sqrt{2\pi\sigma_B^2}} \exp \left[- \frac{1}{2\sigma_B^2} \left(\sum_{j=0}^{p} a_j x_{n-j} \right)^2 \right] \right.$$

$$\left. + \frac{\varepsilon}{\sqrt{2\pi\sigma_I^2}} \exp \left[- \frac{1}{2\sigma_I^2} \left(\sum_{j=0}^{p} a_j x_{n-j} \right)^2 \right] \right]$$

From (13), $u_n = \sum_{j=0}^{p} a_j x_{n-j}$ (A-1a)

Let $E_B(u_n) = \frac{1}{\sqrt{2\pi\sigma_B^2}} \exp \left[- \frac{1}{2\sigma_B^2} u_n^2 \right]$ (A-1b)

$E_I(u_n) = \frac{1}{\sqrt{2\pi\sigma_I^2}} \exp \left[- \frac{1}{2\sigma_I^2} u_n^2 \right]$ (A-1c)

$F_B(u_n) = (1-\varepsilon) E_B(u_n)$ (A-1d)

$F_I(u_n) = \varepsilon E_I(u_n)$ (A-1e)

Then $\ln f = \sum_{n=p+1}^{N} \ln [F_B(u_n) + F_I(u_n)]$ (A-2)

$$\text{Hence} \quad \frac{\partial \ln f}{\partial a_j} = \sum_{n=p+1}^{N} \frac{\frac{\partial}{\partial a_j}\left[F_B(u_n) + F_I(u_n) \right]}{F_B(u_n) + F_I(u_n)}$$

$$= \sum_{n=p+1}^{N} \frac{-\frac{1}{\sigma_B^2} F_B(u_n) - \frac{1}{\sigma_I^2} F_I(u_n)}{F_B(u_n) + F_I(u_n)} u_n \frac{\partial u_n}{\partial a_j}$$

$$\text{ie,} \quad \frac{\partial \ln f}{\partial a_j} = - \sum_{n=p+1}^{N} u_n x_{n-j} \frac{F_B(u_n)/\sigma_B^2 + F_I(u_n)/\sigma_I^2}{F_B(u_n) + F_I(u_n)} \qquad \text{(A-3)}$$

$$\text{Noting} \qquad \sigma^2 = (1-\varepsilon)\sigma_B^2 + \varepsilon\sigma_I^2 = \sigma_B^2 + \varepsilon(\sigma_I^2 - \sigma_B^2)$$

$$\text{it follows that} \quad \frac{\partial \varepsilon}{\partial \sigma^2} = \frac{1}{\sigma_I^2 - \sigma_B^2}$$

$$\frac{\partial \ln f}{\partial \sigma^2} = \frac{1}{\sigma_I^2 - \sigma_B^2} \cdot \frac{\partial \ln f}{\partial \varepsilon} = \frac{1}{\sigma_B^2 - \sigma_I^2} \cdot \sum_{n=p+1}^{N} \frac{-E_B(u_n) + E_I(u_n)}{F_B(u_n) + F_I(u_n)} \qquad \text{(A-4)}$$

$$\frac{\partial^2 \ln f}{\partial a_k \partial a_j} = - \sum_{n=p+1}^{N} x_{n-k} x_{n-j} \frac{\frac{F_B(u_n)}{\sigma_B^2} + \frac{F_I(u_n)}{\sigma_I^2}}{F_B(u_n) + F_I(u_n)} - \sum_{n=p+1}^{N} u_n x_{n-k} \frac{\partial}{\partial a_k}\left[\frac{\frac{F_B(u_n)}{\sigma_B^2} + \frac{F_I(u_n)}{\sigma_I^2}}{F_B(u_n) + F_I(u_n)} \right]$$

$$\text{Let } F_B(u_n)/\sigma_B^2 + F_I(u_n)/\sigma_I^2 = T(u_n)$$

$$F_B(u_n) + F_I(u_n) = B(u_n)$$

$$\frac{\partial T(u_n)}{\partial a_k} = \frac{F_B(u_n)}{\sigma_B^2} \cdot \left[- \frac{u_n}{\sigma_B^2} \frac{\partial u_n}{\partial a_k} \right] + \frac{F_I(u_n)}{\sigma_I^2} \cdot \left[- \frac{u_n}{\sigma_I^2} \frac{\partial u_n}{\partial a_k} \right]$$

$$= - u_n x_{n-k} \left[F_B(u_n)/\sigma_B^2 + F_I(u_n)/\sigma_I^2 \right]$$

$$\frac{\partial B(u_n)}{\partial a_k} = F_B(u_n)\left[-\frac{u_n}{\sigma_B^2}\cdot\frac{\partial u_n}{\partial a_k}\right] + F_I(u_n)\left[-\frac{u_n}{\sigma_I^2}\cdot\frac{\partial u_n}{\partial a_k}\right]$$

$$= -u_k x_{n-k}\left[F_B(u_n)/\sigma_B^2 + F_I(u_n)/\sigma_I^2\right]$$

$$\frac{\partial}{\partial a_k}\frac{T(u_n)}{B(u_n)} = \frac{B(u_n)\dfrac{\partial T(u_n)}{\partial a_k} - T(u_n)\dfrac{\partial B(u_n)}{\partial a_k}}{B(u_n)^2}$$

$$= -\frac{u_n x_{n-k}}{B(u_n)^2}\left[\left[F_B(u_n)+F_I(u_n)\right]\left[\frac{F_B(u_n)}{\sigma_B^4}+\frac{F_I(u_n)}{\sigma_I^4}\right] - \left[\frac{F_B(u_n)}{\sigma_B^2}+\frac{F_I(u_n)}{\sigma_I^2}\right]\right]$$

$$= -\frac{u_n x_{n-k}}{B(u_n)^2}\left[\frac{F_B(u_n)F_I(u_n)}{\sigma_B^4}+\frac{F_B(u_n)F_I(u_n)}{\sigma_I^4}-2\frac{F_B(u_n)F_I(u_n)}{\sigma_B^2\sigma_I^2}\right]$$

$$= -u_n x_{n-k}F_B(u_n)F_I(u_n)\left[\frac{1/\sigma_B^2 - 1/\sigma_I^2}{F_B(u_n)+F_I(u_n)}\right]^2$$

Therefore $\dfrac{\partial^2 \ln f}{\partial a_k \partial a_j}$

$$= -\sum_{n=p+1}^{N} x_{n-j}x_{n-k}\left[\frac{\dfrac{F_B(u_n)}{\sigma_B^2}+\dfrac{F_I(u_n)}{\sigma_I^2}}{F_B(u_n)+F_I(u_n)} - u_n^2\left[\frac{1}{\sigma_B^2}-\frac{1}{\sigma_I^2}\right]\frac{F_B(u_n).F_I(u_n)}{\left[F_B(u_n)+F_I(u_n)\right]^2}\right] \quad (A\text{-}5)$$

$$\frac{\partial^2 \ln f}{\partial \sigma^{2^2}} = \frac{1}{(\sigma_I^2-\sigma_B^2)^2}\frac{\partial}{\partial e}\left[\sum_{n=p+1}^{N}\frac{-E_B(u_n)+E_I(u_n)}{F_B(u_n)+F_I(u_n)}\right]$$

$$\text{ie, } \frac{\partial^2 \ln f}{\partial \sigma^{2^2}} = -\frac{1}{(\sigma_I^2-\sigma_B^2)^2}\sum_{n=p+1}^{N}\left[\frac{E_B(u_n)-E_I(u_n)}{F_B(u_n)+F_I(u_n)}\right]^2 \quad (A\text{-}6)$$

$$\frac{\partial^2 \ln f}{\partial \sigma^2 \partial a_j} = \frac{1}{\sigma_I^2 - \sigma_B^2} \sum_{n=p+1}^{N} -u_n x_{n-j} \frac{\partial}{\partial \varepsilon} \left[\frac{\frac{F_B(u_n)}{\sigma_B^2} + \frac{F_I(u_n)}{\sigma_I^2}}{F_B(u_n) + F_I(u_n)} \right]^2$$

$$= \frac{1}{\sigma_B^2 - \sigma_I^2} \sum_{n=p+1}^{N} x_{n-j} u_n \left[\frac{\left[\frac{E_B(u_n)}{\sigma_B^2} - \frac{E_I(u_n)}{\sigma_I^2} \right] \left[F_B(u_n) + F_I(u_n) \right]}{\left[F_B(u_n) + F_I(u_n) \right]^2} \right.$$

$$\left. + \frac{\left[\frac{F_B(u_n)}{\sigma_B^2} + \frac{F_I(u_n)}{\sigma_I^2} \right] \left[E_B(u_n) - E_I(u_n) \right]}{\left[F_B(u_n) + F_I(u_n) \right]^2} \right]$$

It follows that $$\frac{\partial^2 \ln f}{\partial \sigma^2 \partial a_j} = \sum_{n=p+1}^{N} x_{n-j} u_n \frac{1}{\sigma_I^2 \sigma_B^2} \cdot \frac{E_B(u_n)\, E_I(u_n)}{\left[F_B(u_n) + F_I(u_n)^2 \right]} \qquad \text{(A-7)}$$

Equations (A-3) to (A-7) completely determine the gradient vector and the Hessian matrix. u_n, $E_1(u_n)$, $E_2(u_n)$, $F_1(u_n)$ and $F_2(u_n)$ need to be computed only once for every n in each iteration and can be used to find all the first and second derivatives.

APPENDIX B

Use of transformation on σ^2

Experiments show a rather weak dependence of the log likelihood function on σ^2 (or equivalently ε). This problem can cause the $(p+1)$-dimensional optimization not to converge. A possible solution is to use some transformation $\eta = g(\varepsilon)$ such that η increases slowly with ε. If a proper transformation is chosen lnf will, hopefully, show a distinct peak when optimized over η. The intuitive idea behind this technique is to increase the sensitivity of the function to the variable over which it is to be optimized. Since g is an increasing function of ε, the optimum value of η will correspond to a unique value of ε. An example of such a transformation is

$$\eta = \varepsilon^r$$

where r is a small fraction. This implies that $\dfrac{\partial \eta}{\partial \varepsilon} = \dfrac{r}{\varepsilon^{1-r}}$

and for any function Q of ε

$$\frac{\partial Q}{\partial \eta} = \frac{\partial Q}{\partial \varepsilon} \cdot \frac{\varepsilon^{1-r}}{r} \tag{B-1}$$

$$\frac{\partial^2 Q}{\partial \eta^2} = \frac{\varepsilon^{1-r}}{r}\left[\frac{\partial^2 Q}{\partial \varepsilon^2} \cdot \frac{\varepsilon^{1-r}}{r} + \frac{\partial Q}{\partial \varepsilon} \cdot (1-r)\frac{\varepsilon^{-r}}{r}\right]$$

$$= \frac{\varepsilon^{1-2r}}{r^2} \left[(1-r) \frac{\partial Q}{\partial \varepsilon} + \varepsilon \frac{\partial^2 Q}{\partial \varepsilon^2} \right] \qquad \text{(B-2)}$$

(B-1) and (B-2) could be used to modify (A-4), (A-6) and (A-7) for optimization over η.

Experimentally, r=0.1 seemed to work for a wide range of ε.

Table I : Parameters of the AR processes used for simulation:

Process	a_1	a_2	a_3	a_4	poles
I	-1.352	1.338	-0.662	0.240	$0.7\exp[j2\pi(0.12)]$ $0.7\exp[j2\pi(0.21)]$
II	-2.760	3.809	-2.654	0.924	$0.98\exp[j2\pi(0.11)]$ $0.98\exp[j2\pi(0.14)]$

Table II : Performance of the Forward-Backward Estimators

		True value	Sample mean	Sample variance	Cramer Rao bound	"Gaussian" C R bound
Process I	a_1	-1.352	-1.3482	1.0197×10^{-3}	1.0491×10^{-4}	9.4618×10^{-4}
	a_2	1.338	1.3326	2.3822×10^{-3}	2.5961×10^{-4}	2.3414×10^{-3}
	a_3	-0.662	-0.6591	2.3531×10^{-3}	2.5961×10^{-4}	2.3414×10^{-3}
	a_4	0.240	0.2382	9.6246×10^{-3}	1.0491×10^{-4}	9.4618×10^{-4}
	σ^2	10.900	10.8315	2.7778	0.3149	0.2386
Process II	a_1	-2.760	-2.7567	1.6569×10^{-4}	1.6278×10^{-5}	1.4681×10^{-4}
	a_2	3.809	3.8001	8.3418×10^{-4}	8.0163×10^{-5}	7.2300×10^{-4}
	a_3	-2.654	-2.6447	8.4388×10^{-4}	8.0163×10^{-5}	7.2300×10^{-4}
	a_4	0.924	0.9197	1.7083×10^{-4}	1.6278×10^{-5}	1.4681×10^{-4}
	σ^2	10.900	10.8315	2.7713	0.3149	0.2386

Table III : Performance of the Maximum Likelihood Estimators

		True value	Sample mean	Sample variance	Cramer Rao bound	"Gaussian" C R bound
Process I	a_1	-1.352	-1.3527	1.0219×10^{-4}	1.0491×10^{-4}	9.4618×10^{-4}
	a_2	1.338	1.3391	2.4619×10^{-4}	2.5961×10^{-4}	2.3414×10^{-3}
	a_3	-0.662	-0.6629	2.4253×10^{-4}	2.5961×10^{-4}	2.3414×10^{-3}
	a_4	0.240	0.2404	1.0352×10^{-4}	1.0491×10^{-4}	9.4618×10^{-4}
	σ^2	10.900	10.8544	1.2061	0.3149	0.2386
Process II	a_1	-2.760	-2.7597	1.7588×10^{-5}	1.6278×10^{-5}	1.4681×10^{-4}
	a_2	3.809	3.8081	9.0671×10^{-5}	8.0163×10^{-5}	7.2300×10^{-4}
	a_3	-2.654	-2.6531	9.1796×10^{-5}	8.0163×10^{-5}	7.2300×10^{-4}
	a_4	0.924	0.9236	1.8545×10^{-5}	1.6278×10^{-5}	1.4681×10^{-4}
	σ^2	10.900	10.8454	1.1990	0.3149	0.2386

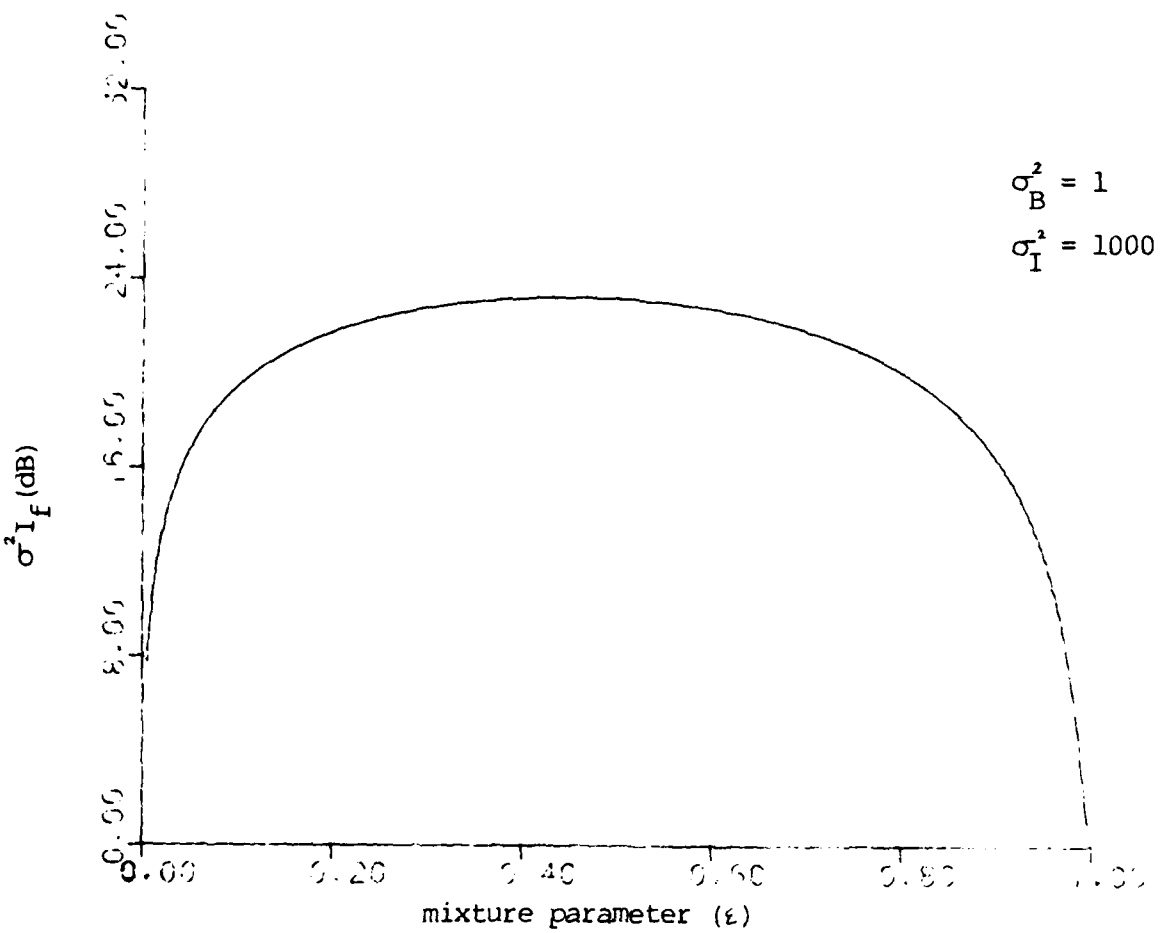

Figure 1(a). Degree of non-Gaussianity of mixed-Gaussian PDF

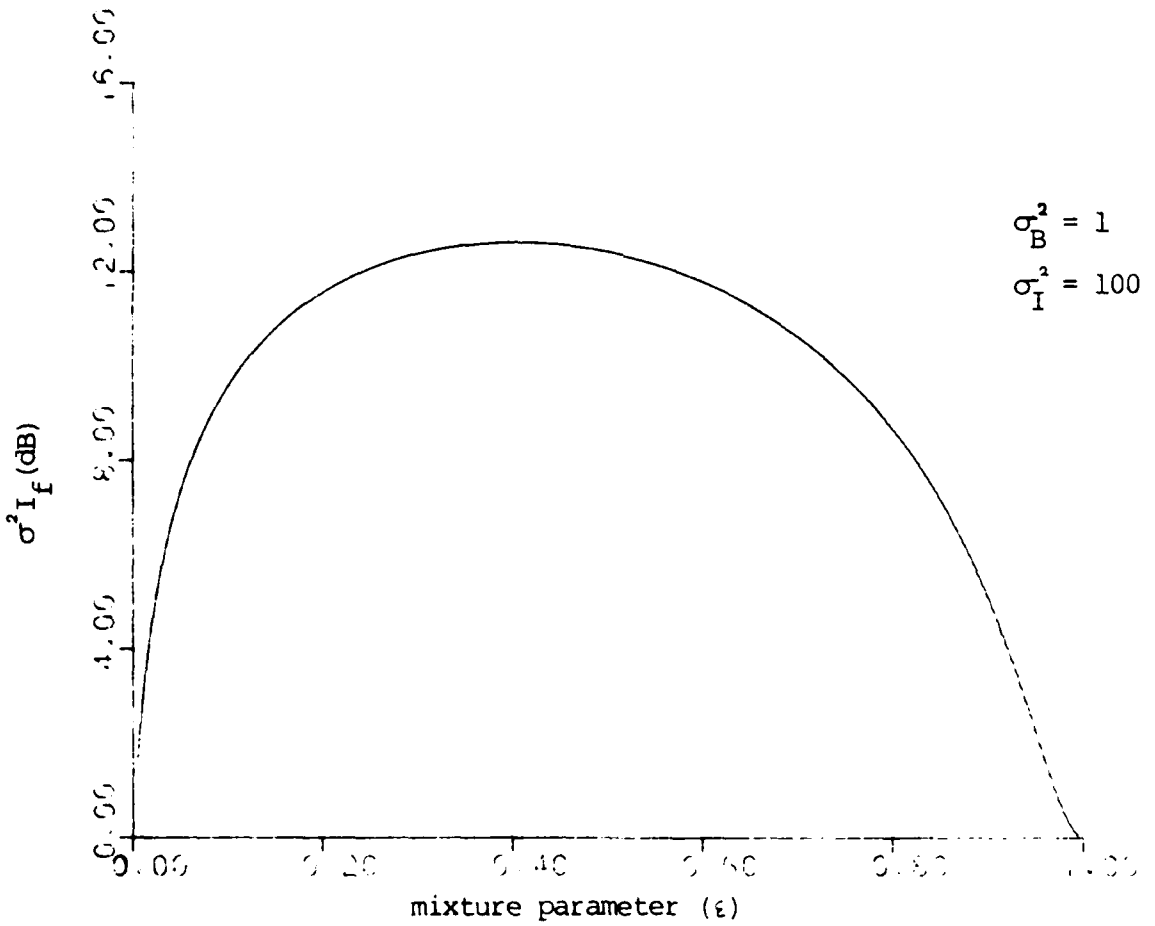

Figure 1(b). Degree of non-Gaussianity of mixed-Gaussian PDF

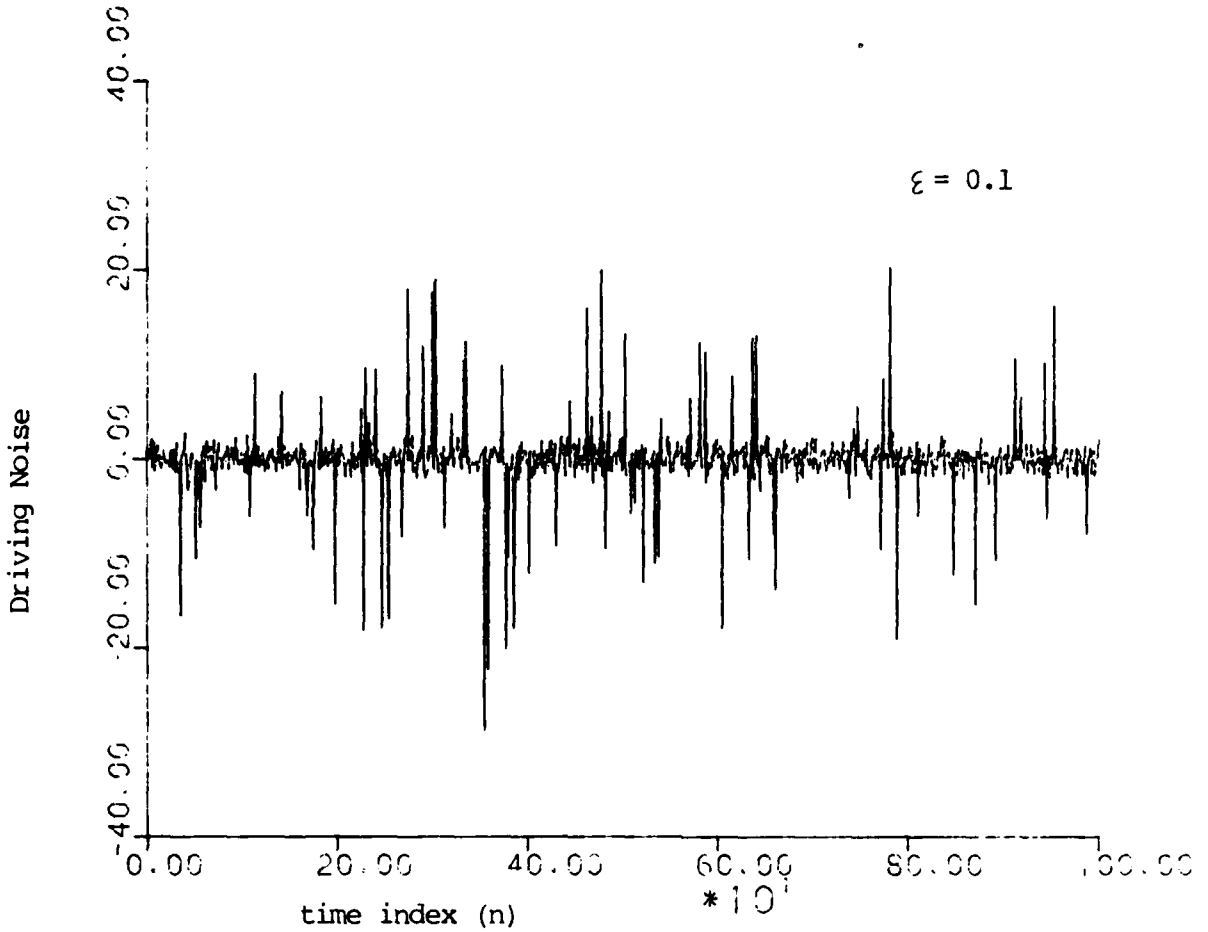

(a) Input

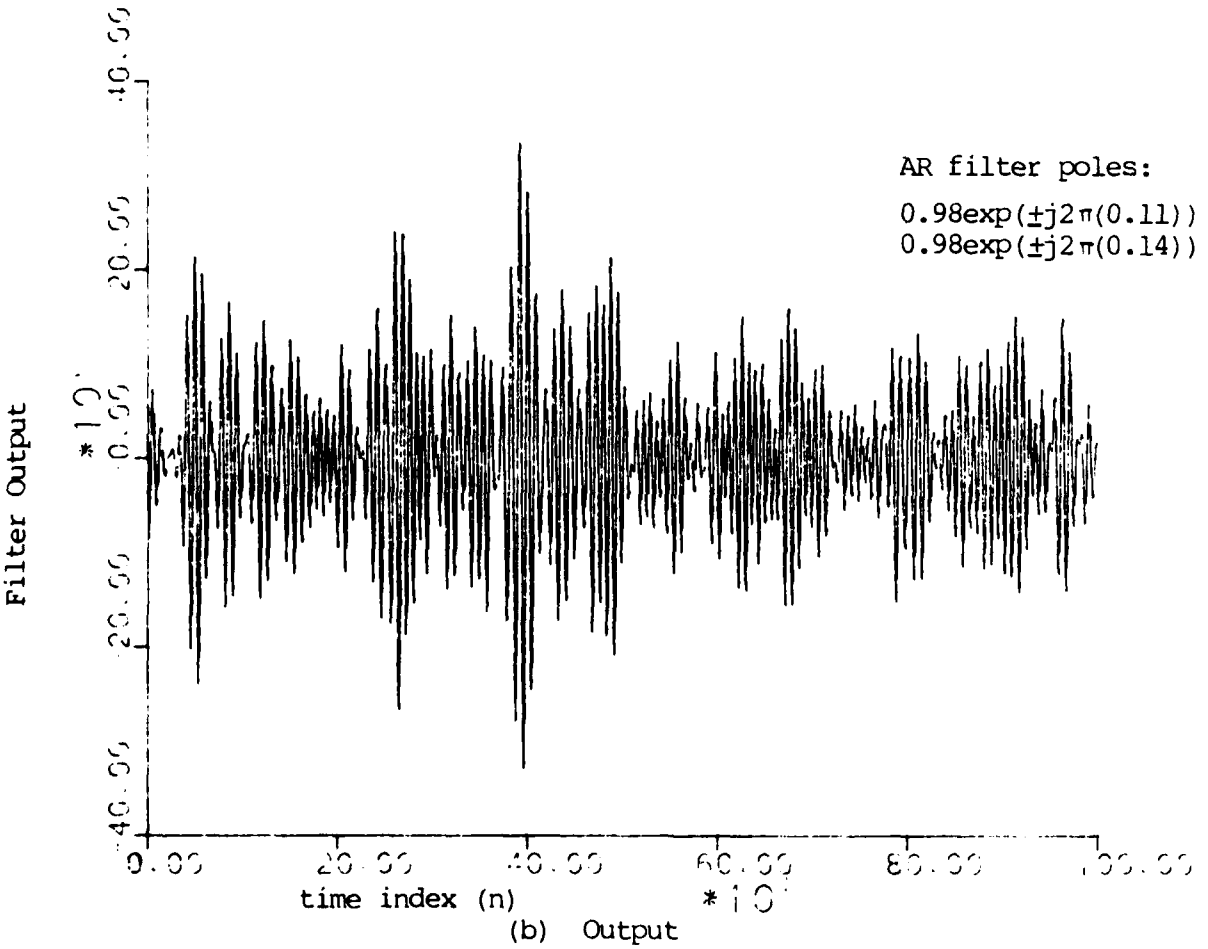

(b) Output

Figure 2. Mixed-Gaussian time series at the input and output of an AR filter

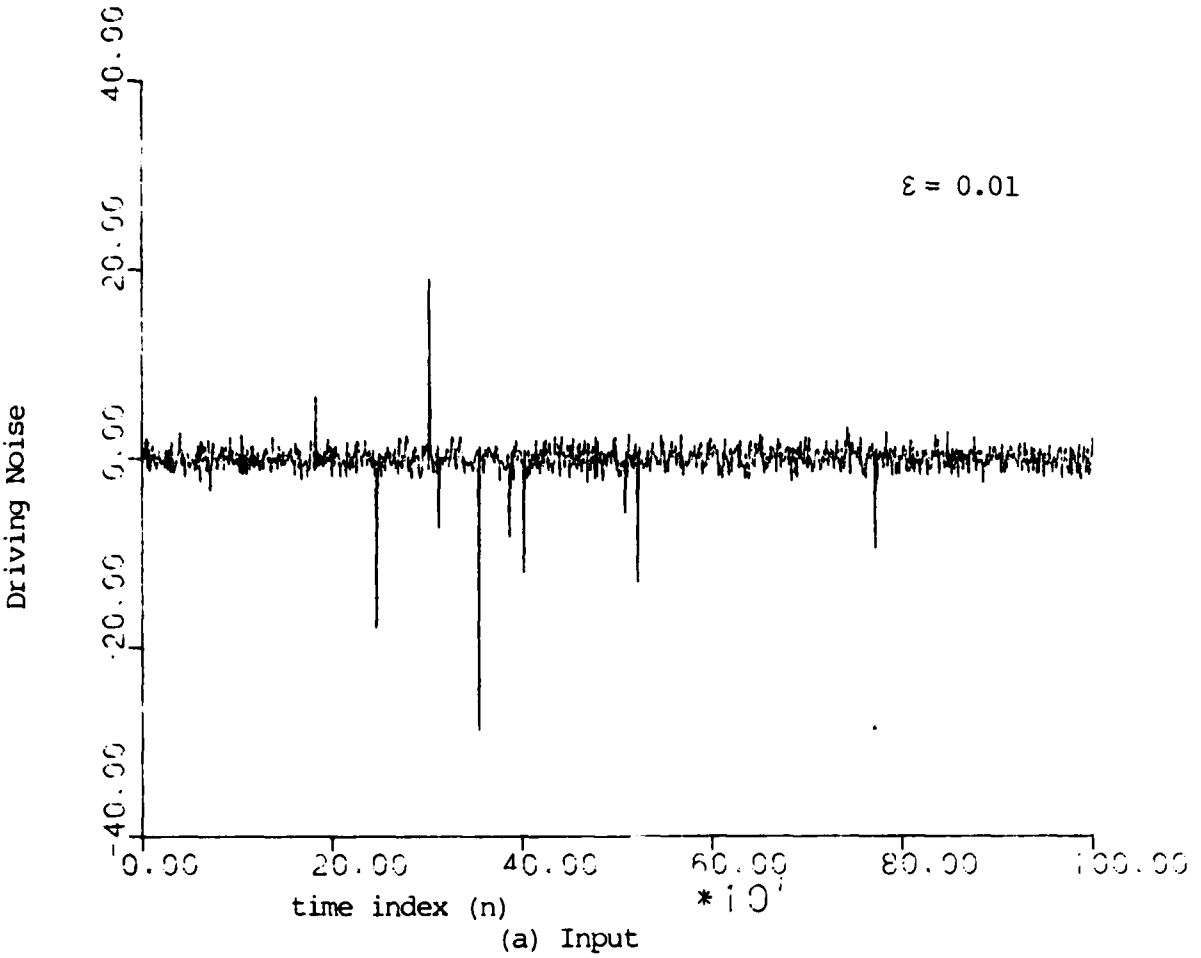

(a) Input

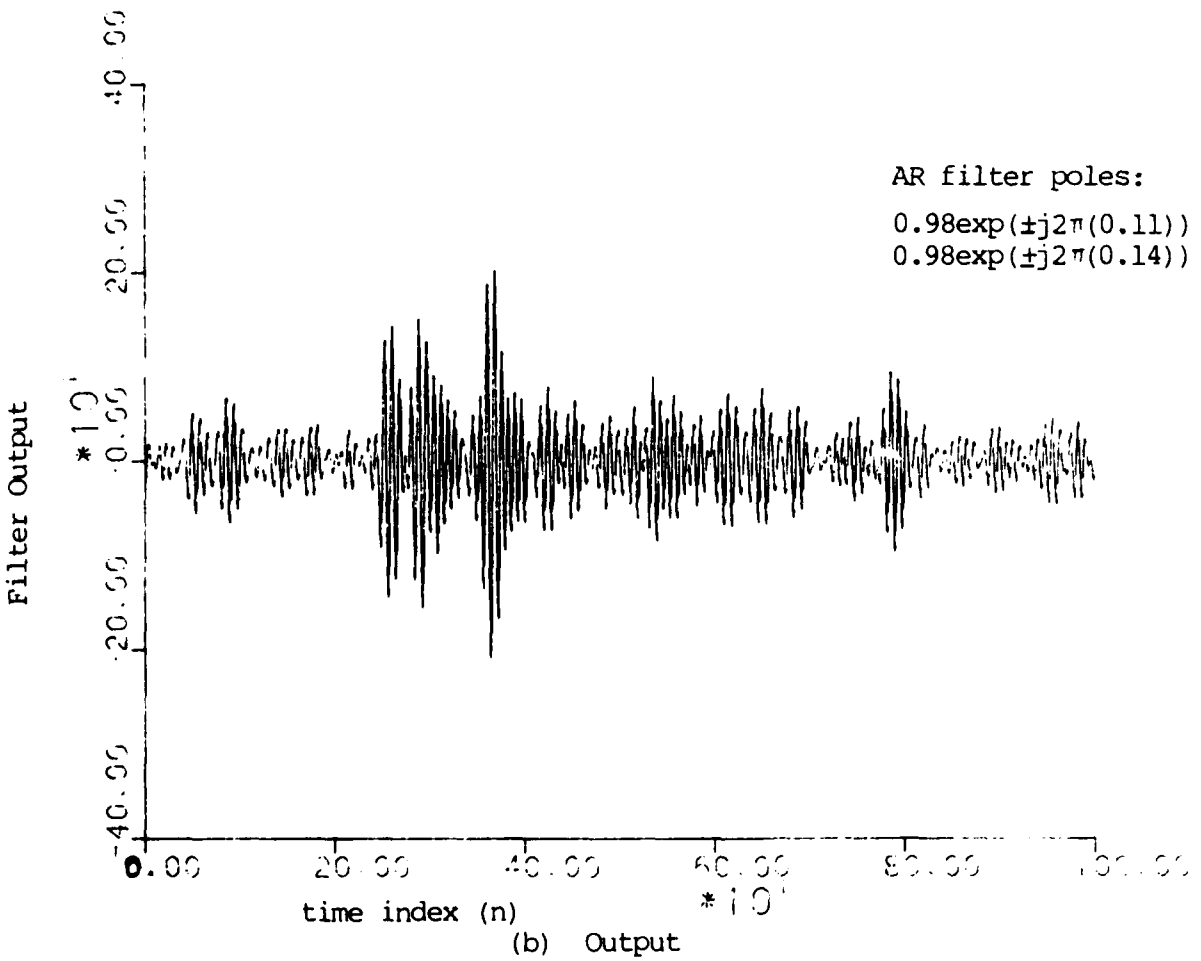

(b) Output

Figure 3. Mixed-Gaussian time series at the input and output of an AR filter

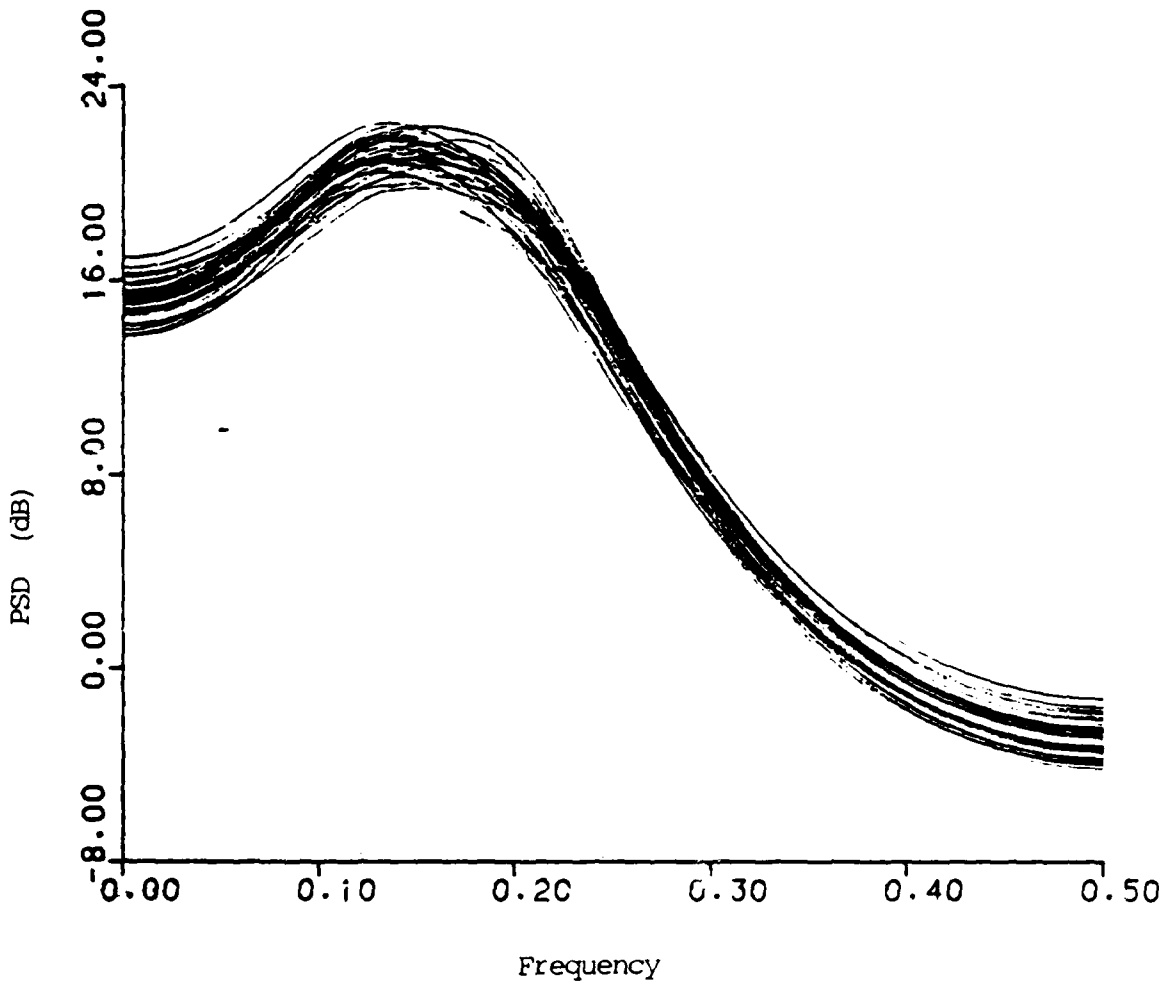

Figure 4(a). Forward/backward PSD estimates of process I

(50 estimates overlayed)

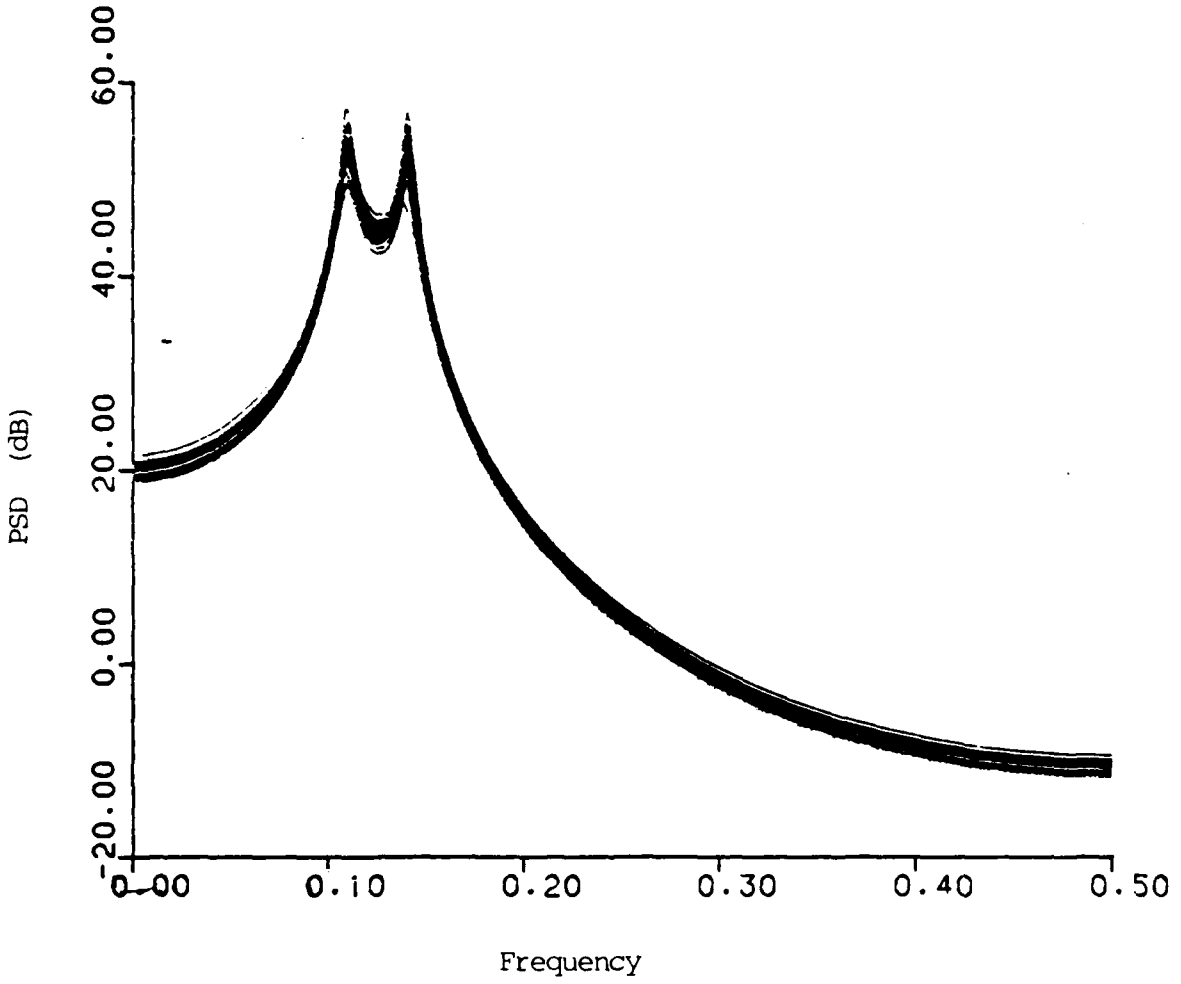

Figure 4(b). Forward/Backward PSD estimates of process II

(50 estimates overlayed)

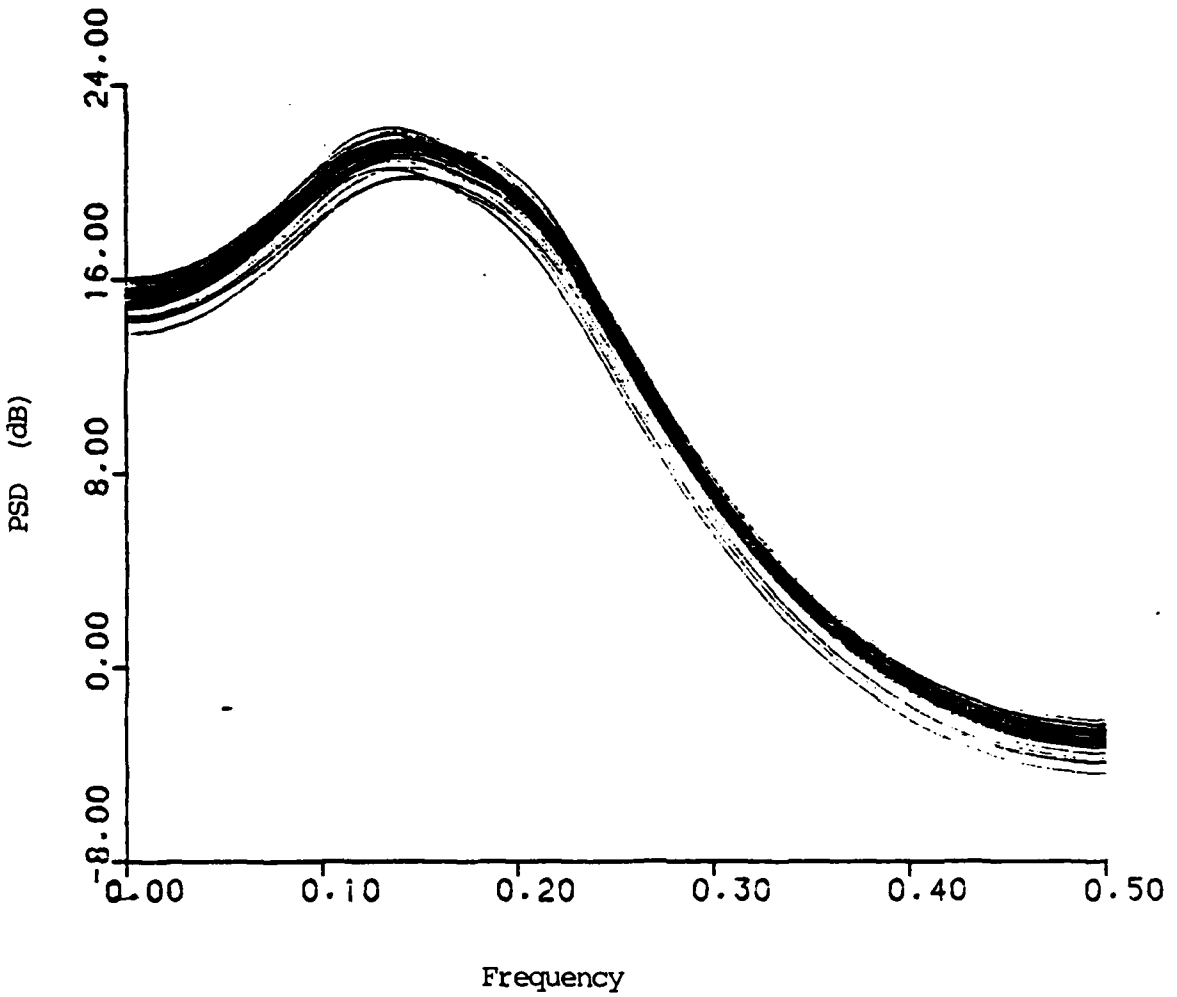

Figure 5(a). Maximum likelihood PSD estimates of process I

(50 estimates overlayed)

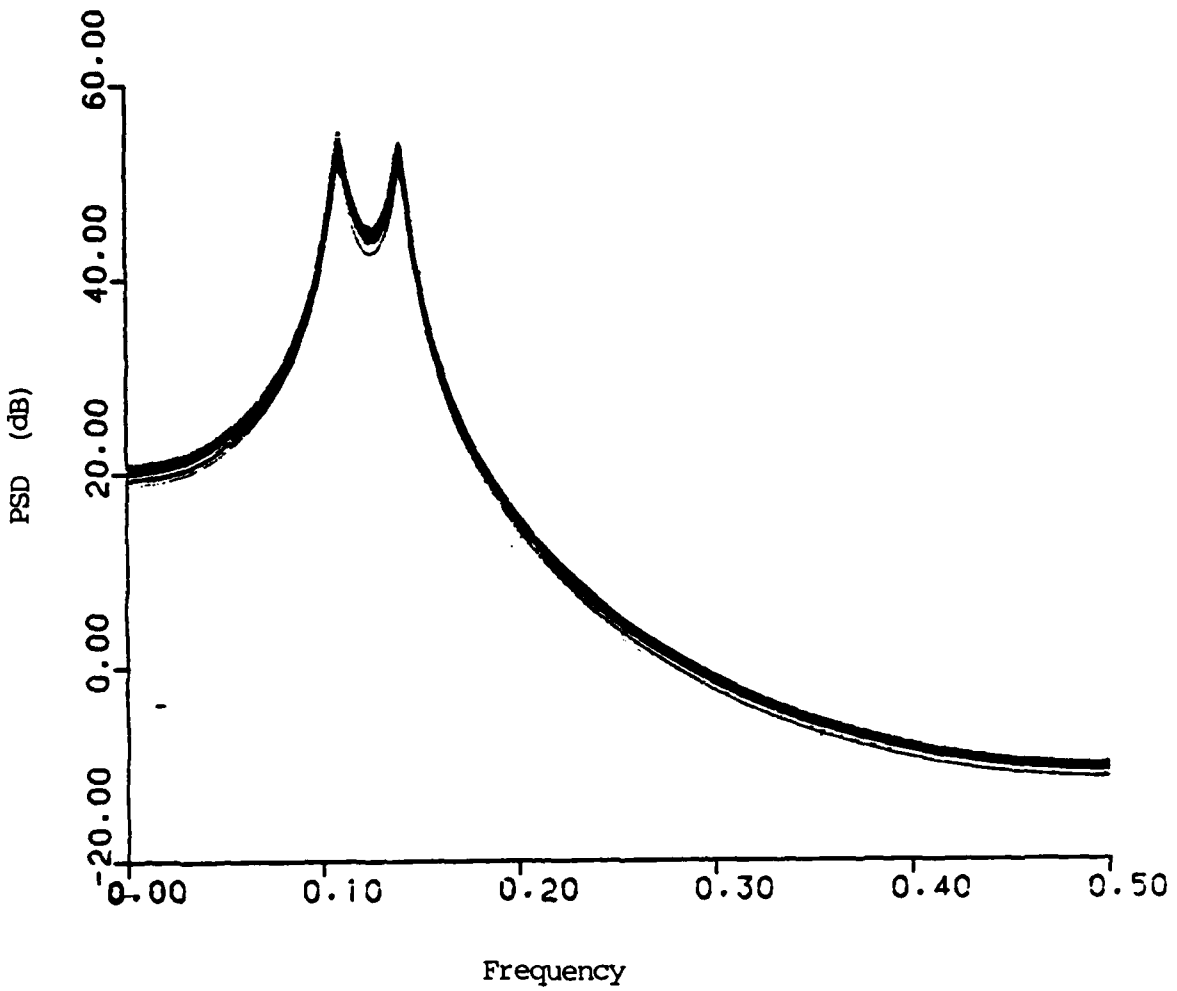

Figure 5(b). Maximum likelihood PSD estimates of process II

(50 estimates overlayed)

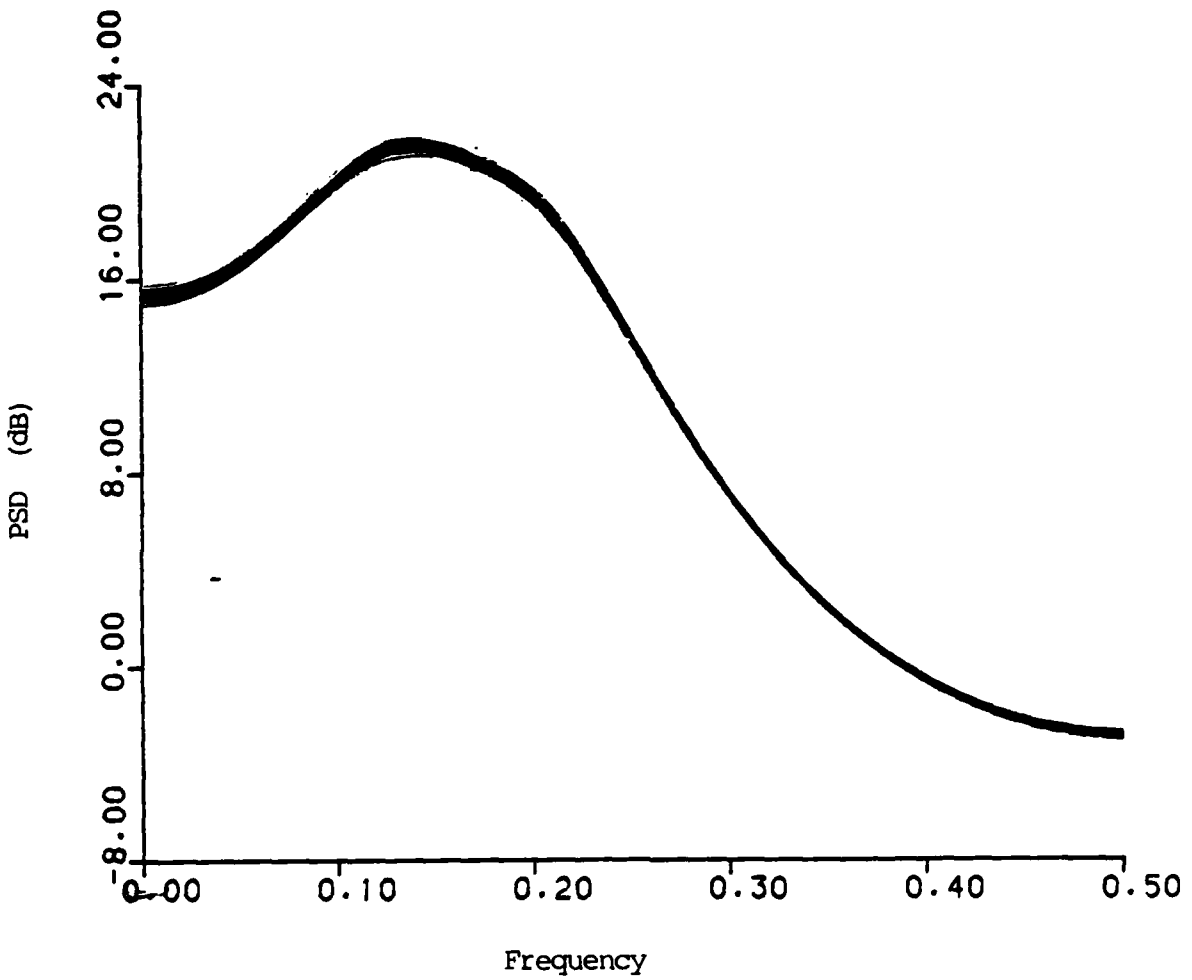

Figure 6(a). Maximum likelihood PSD estimates of process I

(50 estimates overlayed, known value of σ^2 used)

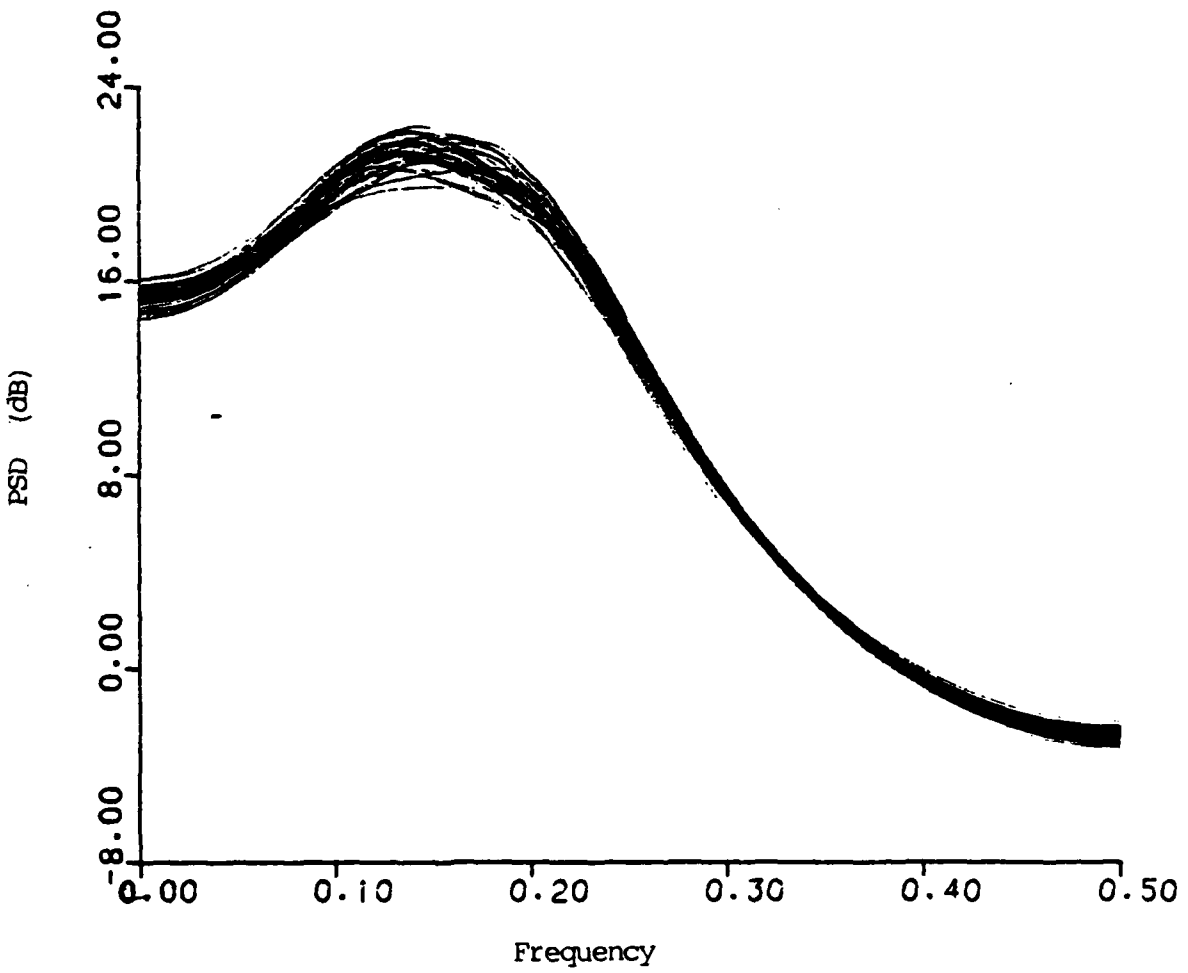

Figure 6(b). Forward/backward PSD estimates of process I

(50 estimates overlayed, known value of σ^2 used)

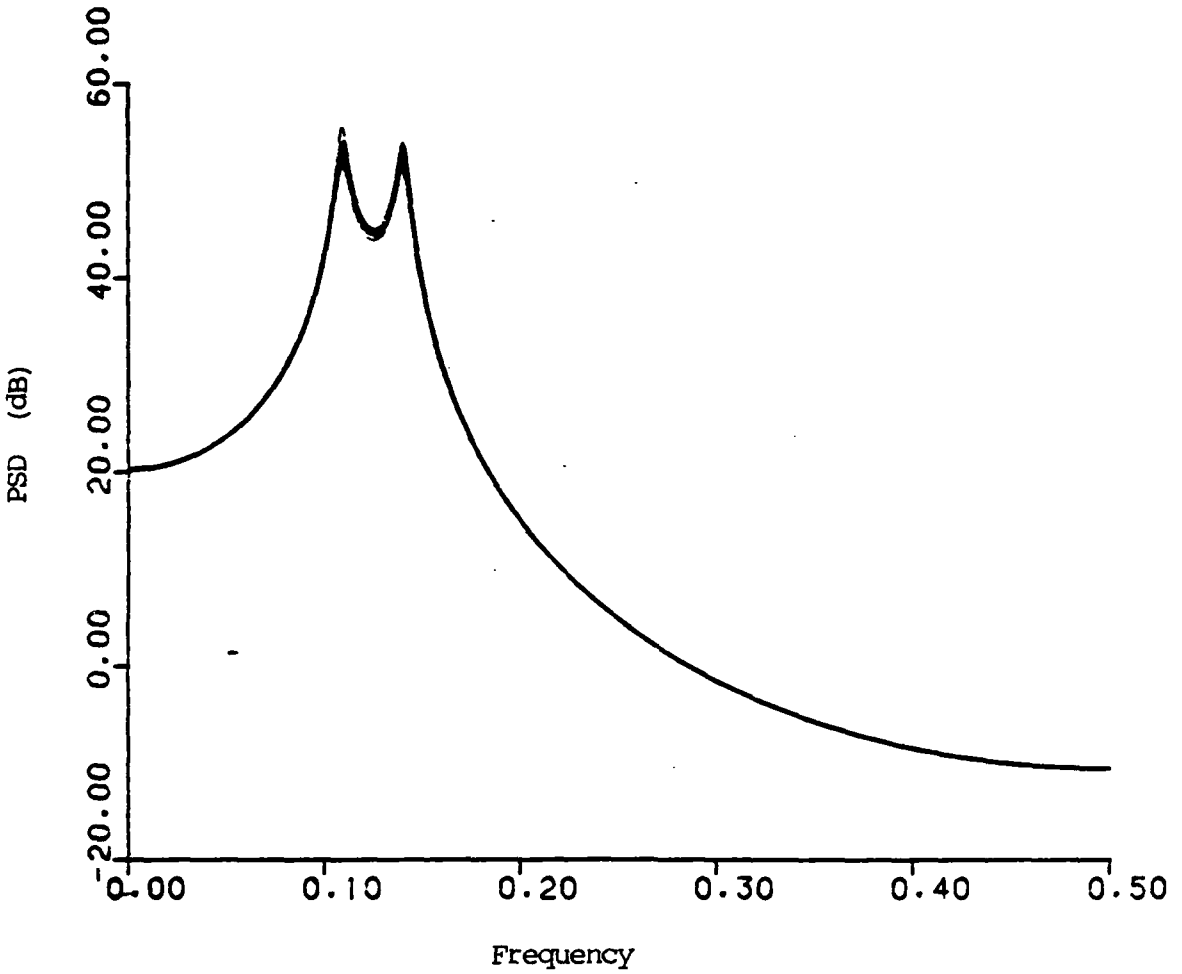

Figure 7(a). Maximum likelihood PSD estimates of process II

(50 estimates overlayed, known value of σ^2 used)

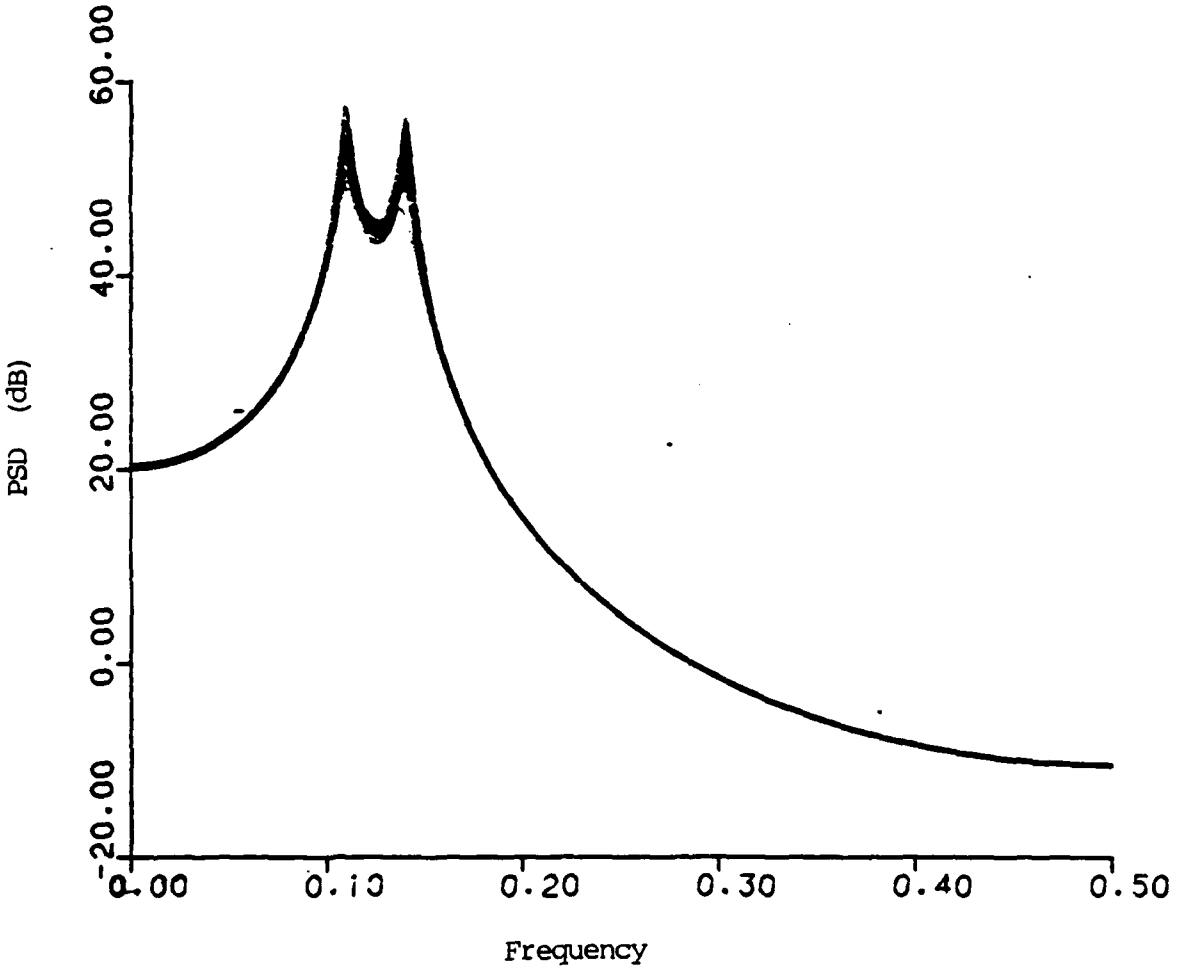

Figure 7(b). Forward/backward PSD estimates of process II

(50 estimates overlayed, known value of σ^2 used)

OFFICE OF NAVAL RESEARCH
STATISTICS AND PROBABILITY PROGRAM

BASIC DISTRIBUTION LIST
FOR
UNCLASSIFIED TECHNICAL REPORTS

FEBRUARY 1982

	Copies
Statistics and Probability Program (Code 411(SP)) Office of Naval Research Arlington, VA 22217	3
Defense Technical Information Center Cameron Station Alexandria, VA 22314	12
Commanding Officer Office of Naval Research Eastern/Central Regional Office Attn: Director for Science Barnes Building 495 Summer Street Boston, MA 02210	1
Commanding Officer Office of Naval Research Western Regional Office Attn: Dr. Richard Lau 1030 East Green Street Pasadena, CA 91101	1
U. S. ONR Liaison Office - Far East Attn: Scientific Director APO San Francisco 96503	1
Applied Mathematics Laboratory David Taylor Naval Ship Research and Development Center Attn: Mr. G. H. Gleissner Bethesda, Maryland 20084	1
Commandant of the Marine Coprs (Code AX) Attn: Dr. A. L. Slafkosky Scientific Advisor Washington, DC 20380	1
Navy Library National Space Technology Laboratory Attn: Navy Librarian Bay St. Louis, MS 39522	1
U. S. Army Research Office P.O. Box 12211 Attn: Dr. J. Chandra Research Triangle Park, NC 27706	1
Director National Security Agency Attn: R51, Dr. Maar Fort Meade, MD 20755	1
ATAA-SL, Library U.S. Army TRADOC Systems Analysis Activity Department of the Army White Sands Missile Range, NM 88002	1
ARI Field Unit-USAREUR Attn: Library c/o ODCSPER HQ USAEREUR & 7th Army APO New York 09403	1
Library, Code 1424 Naval Postgraduate School Monterey, CA 93940	1
Technical Information Division Naval Research Laboratory Washington, DC 20375	1
OASD (I&L), Pentagon Attn: Mr. Charles S. Smith Washington, DC 20301	1

Copies

Director
AMSAA
Attn: DRXSY-MP, H. Cohen
Aberdeen Proving Ground, MD 1
21005

Dr. Gerhard Heiche
Naval Air Systems Command
(NAIR 03)
Jefferson Plaza No. 1
Arlington, VA 20360 1

Dr. Barbara Bailar
Associate Director, Statistical
Standards
Bureau of Census
Washington, DC 20233 1

Leon Slavin
Naval Sea Systems Command
(NSEA 05H)
Crystal Mall #4, Rm. 129
Washington, DC 20036 1

B. E. Clark
RR #2, Box 647-B
Graham, NC 27253 1

Naval Underwater Systems Center
Attn: Dr. Derrill J. Bordelon
Code 601
Newport, Rhode Island 02840 1

Naval Coastal Systems Center
Code 741
Attn: Mr. C. M. Bennett
Panama City, FL 32401 1

Naval Electronic Systems Command
(NELEX 612)
Attn: John Schuster
National Center No. 1
Arlington, VA 20360 1

Defense Logistics Studies
Information Exchange
Army Logistics Management Center
Attn: Mr. J. Dowling
Fort Lee, VA 23801 1

Copies

Reliability Analysis Center (RAC)
RADC/RBRAC
Attn: I. L. Krulac
Data Coordinator/
Government Programs
Griffiss AFB, New York 13441 1

Technical Library
Naval Ordnance Station
Indian Head, MD 20640 1

Library
Naval Ocean Systems Center
San Diego, CA 92152 1

Technical Library
Bureau of Naval Personnel
Department of the Navy
Washington, DC 20370 1

Mr. Dan Leonard
Code 8105
Naval Ocean Systems Center
San Diego, CA 92152 1

Dr. Alan F. Petty
Code 7930
Naval Research Laboratory
Washington, DC 20375 1

Dr. M. J. Fischer
Defense Communications Agency
Defense Communications Engineering
Center
1860 Wiehle Avenue
Reston, VA 22090 1

Mr. Jim Gates
Code 9211
Fleet Material Support Office
U. S. Navy Supply Center
Mechanicsburg, PA 17055 1

Mr. Ted Tupper
Code M-311C
Military Sealift Command
Department of the Navy
Washington, DC 20390 1

	Copies		Copies
Mr. F. R. Del Priori Code 224 Operational Test and Evaluation Force (OPTEVFOR) Norfolk, VA 23511	1		

END

DTIC

9-86